Resonance magnetic x-ray-scattering study of erbium

M. K. Sanyal* and Doon Gibbs
Department of Physics, Brookhaven National Laboratory, Upton, New York 11973

J. Bohr and M. Wulff†
Risø National Laboratory, DK-4000 Roskilde, Copenhagen, Denmark

(Received 18 June 1993)

The magnetic phases of erbium have been studied by resonance x-ray-scattering techniques. When the incident x-ray energy is tuned near the L_{III} absorption edge, large resonant enhancements of the magnetic scattering are observed above 18 K. We have measured the energy and polarization dependence of this magnetic scattering and analyzed it using a simple model based on electric dipole and quadrupole transitions among atomic orbitals. The line shapes can be fitted to a magnetic structure combining both c-axis-modulated and basal-plane components. Below 18 K, we have observed unusual behavior of the magnetic scattering as a function of energy, whose origin is not understood.

I. INTRODUCTION

The magnetic structure of erbium stabilizes in a variety of different phases as a function of temperature. The complex structures of these phases have been addressed in a series of neutron[1-4] and x-ray scattering [5-6] studies and new interesting features continue to be discovered.[7-8] In this paper, we present the results of a study of the polarization and resonance properties of x-ray magnetic scattering from a single crystal of erbium. The polarization and energy dependence of the line shapes have been characterized as a function of the temperature and analyzed in terms of a simple resonance model using dipole and quadrupole excitations coupling $2p$ to $5d$ and $4f$ atomic orbitals.[9-12] We have fitted the energy dependence of the line shapes to a model of the magnetic structure in which the average tilt angle of the moments away from the c axis is allowed to change with the temperature. In the so-called conical phase below 18 K we have observed unusual energy and polarization dependence of the magnetic scattering, whose origin is not understood.

Erbium has a hcp crystal structure with two atomic layers per chemical unit cell and a saturation magnetic moment of $9\mu_B$/atom. In the ground state there are 11 $4f$ electrons in a Hund's rule $4F_{15/2}$ configuration and three electrons in the $5d$ and $6(s-p)$ bands. Neutron-diffraction studies have identified three distinct regions of magnetic order in erbium.[2,3] Below the Néel temperature of about 89 K and above 52 K, the moments are believed to be ordered along the c axis and modulated with an incommensurate wavelength close to seven layers. For temperatures between 52 and 18 K, an additional component of the magnetization density develops within the basal plane, forming a magnetic structure with a unique chirality. In earlier studies,[2,3] the period of this basal plane magnetic modulation was found to be identical to that of the c-axis modulation. Recently, a new magnetic structure, called a wobbly cycloid, has been proposed[8] for erbium. In this model, the magnetic moments are confined mainly to the c-a plane, but also exhibit a small b-axis component with a slightly different magnetic wave vector. As the temperature is lowered to 22 K, additional odd harmonics of order up to 21 have been observed by neutron diffraction.[2,8] The temperature dependence of the modulation wave vector has been studied using both neutron and x-ray diffraction.[2,4,5,8] In high-resolution x-ray-scattering studies,[5,6] the magnetic wave vector was found to decrease with temperature below 52 K and to exhibit a sequence of lock-in transformations to commensurate values. These observations have recently been confirmed in two neutron-scattering studies.[4,8] Additional charge scattering was observed at $2\tau_m$, as well as at satellite positions split symmetrically about the magnetic scattering at τ_m. The latter peaks were ascribed to spin-slip scattering[5,6] in erbium. Below 18 K, there is a first-order transformation to a commensurate magnetic structure (with $\tau_m = \frac{5}{21}$) which is believed to be a conical phase.

II. EXPERIMENTAL DETAILS

The experiments were performed on beamline X22C at the National Synchrotron Light Source (NSLS). This beamline utilizes a doubly focusing nickel-coated mirror and a fixed-exit Ge(111) double-crystal monochromator.[12] A single crystal ($9\times4\times3$ mm^3) of erbium grown at Ames Laboratory was mounted in a variable-temperature displex and the experiments performed in a reflection geometry. The coordinate system was chosen in such a way that the σ-polarized components of the incident and scattered beams were normal to the vertical diffraction plane, while the π-polarized components (rotated by 90°) lay within the diffraction plane. In this geometry the incident polarization is predominantly σ-polarized with a degree of linear polarization, defined as

$$P=(I_\sigma^0-I_\pi^0)/(I_\sigma^0+I_\pi^0)\ , \tag{1}$$

equal to 0.94. In Eq. (1), I_σ^0 and I_π^0 represent the σ- and π-polarized intensities of the incident beam.

Linear polarization analysis of the scattered beam was performed using a pyrolytic-graphite (PG) crystal, as has been described previously.[12,13] We can write down expressions for the measured intensities of the scattered beam in the σ and π channels of the polarization analyzer as follows:

$$I_\sigma=|(f_{\sigma-\sigma}+f_{\pi-\sigma})|^2+\cos^2(2\phi)|(f_{\sigma-\pi}+f_{\pi-\pi})|^2 \tag{2}$$

and

$$I_\pi=|(f_{\sigma-\pi}+f_{\pi-\pi})|^2+\cos^2(2\phi)|(f_{\sigma-\sigma}+f_{\pi-\sigma})|^2\ , \tag{3}$$

where a typical scattering amplitude like $f_{\sigma\text{-}\pi}$ indicates the scattering of photons from a σ-polarized state to a π-polarized final state. All these cross sections can be calculated by considering only the linearly polarized components of the scattering and using known equations.[10,14] In the above equations, the terms containing $\cos^2(2\phi)$, where 2ϕ is the scattering angle of the polarization analyzer crystal, indicate the "leakage" of one polarization component of the scattered photons into the other channel. It should be mentioned in this regard that the PG(006) reflection, which we used in the analyzer, gives a scattering angle of 90° at an incident of energy 7847 eV. Near the $L_{\rm III}$ absorption edge of erbium (8358eV), the scattering angle becomes 83.2°, and so a small leakage is expected. For resonant charge scattering, the σ-π and π-σ components are small compared to the σ-σ and π-π components. Then, we can write the pure charge scattering intensity in the π channel by neglecting the π-π scattering as compared to the strong σ-σ scattering in Eq. (2) as

$$I_\pi=|f_{\pi\text{-}\pi}|^2+\cos^2(2\phi)I_\sigma\ . \tag{4}$$

The second term of Eq. (4) represents a leakage intensity of the order of 1% of the intensity of the σ component for pure charge scattering peaks. This leakage intensity will be observed in the π channel along with the π-π component allowed for the pure charge scattering [given by the first term of Eq. (4)]. The intensity of the π-π scattering near the (0, 0, 2) reflection of erbium is expected to be around 4% of the intensity of the σ-σ scattering (calculated using a degree of linear polarization of 0.94 for the incident beam).

The σ-σ and σ-π components of the scattering from typical l scans taken around the magnetic peak at 40 K for incident x-ray energies tuned near and away from the $L_{\rm III}$ absorption edge (8358eV) of erbium are shown in Fig. 1. There are peaks observed at wave vectors $(2+\tau_s)=2.105c^*\simeq(2+\frac{2}{15})c^*$, $(2+\tau_m)=2.267c^*\simeq(2+\frac{4}{15})c^*$, and $(2+2\tau_m)=2.534c^*$. τ_s and τ_m correspond to the spin-slip and magnetic wave vectors,[5,6] respectively. The decrease in intensity of the scattering

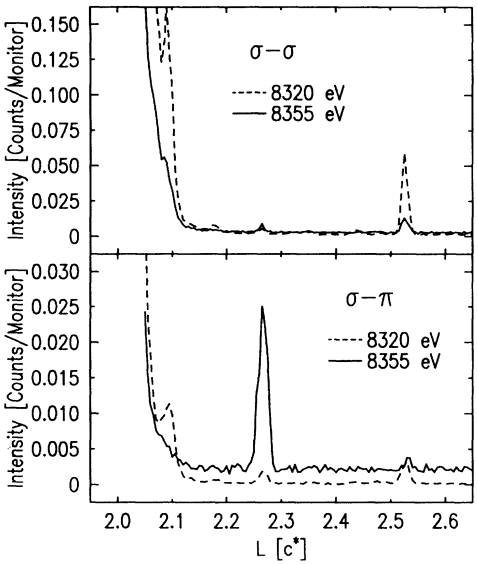

FIG. 1. Scans of σ-polarized (top) and π-polarized (bottom) components of the scattered beam taken along the $[0,0,L]$ direction at 40 K for two energies near and below the $L_{\rm III}$ absorption edge (8358 eV) of erbium.

near the absorption edge both at $2\tau_m$ and at τ_s in the σ-σ channel is characteristic of charge scattering. The π component of the slip scattering peak at τ_s arises from the leakage of the σ component into the π channel and from the π-π scattering, as discussed above. The ratio of the background subtracted peak intensities at τ_s for the π and σ components turns out to be 0.06, consistent with the value expected from Eq. (4). It is to be noted that the ratio of intensities of the π and σ components at $2\tau_m$ is also 0.06 indicating that the peak at this wave vector probably arises mainly from charge scattering.

The enhancement of the magnetic scattering at τ_m occurs mostly, as observed earlier,[9-12] in the σ-π channel (see Fig. 1). The intensity of the magnetic peak at τ_m increases from 15 counts per s to 200 counts per s in the σ-π channel as the energy is changed from 8320 to 8355 eV at a temperature of 40 K (and an electron beam current of 150 mA in the storage ring).

We plot in Fig. 2 the energy dependence of the background intensity (mainly fluorescence) along with the integrated magnetic scattering intensity measured at $(0,0,2+\tau_m)$. The raw data shown in Fig. 2 were taken at 78 K in the c-axis-modulated phase without polarization analysis. Note that the peak of the magnetic scattering occurs at the inflection point of the fluorescence intensity, which provides a continuous on-line calibration of the incident x-ray energy during the experiment. In the Appendix we describe how the absorption coefficient μ as a function of energy near the $L_{\rm III}$ absorption edge can be estimated from the fluorescence data for the purpose of making an absorption correction. We checked this method of calculation using a data set of holmium, for which the transmission through a 5-μm film and the fluorescence were measured simultaneously. This is also

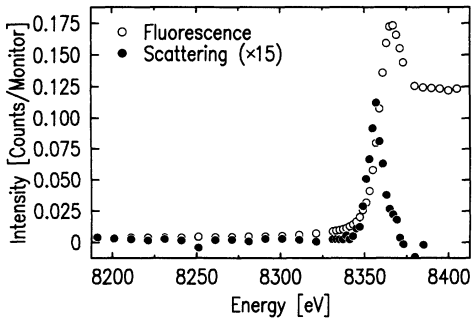

FIG. 2. The integrated and background intensities (fluorescence) of the $(0,0,2+\tau_m)$ reflection at 78 K as the incident x-ray energy is tuned through the L_{III} edge.

discussed in the Appendix. The resultant agreement with the measured absorption coefficient is satisfactory, at least for the qualitative analysis described in this paper.

The absorption coefficients, calculated using the method described in the Appendix, were used to correct the magnetic scattering intensities in all the subsequent fitting. For simplicity, we have assumed the infinite flat plate geometry, in which the integrated intensity is multiplied by the absorption coefficient μ at each incident photon energy. In Fig. 3, we show the integrated intensities measured for the $(0,0,2+\tau_m)$ and $(0,0,4+\tau_m)$ magnetic satellites obtained at temperatures of 40 and 64 K. The data in the figures have been corrected at each energy for the erbium absorption. It is important to note that none of the qualitative features of the line shapes visible in the raw data (see Fig. 2) is significantly altered by the absorption correction. After correction for the absorption, the integrated intensity measured at the L_{III} edge for the $(0,0,2+\tau_m)$ reflection at 40 K is greater by a factor of about 40 than the integrated intensity measured at 8200 eV. In the energy-dependent line shapes of the magnetic scattering in holmium,[9,10,12] there was observed an asymmetric tail on the low-energy side for the $(0,0,2+\tau_m)$ and $(0,0,4+\tau_m)$ satellites, which arose from the interference of the resonant and nonresonant amplitudes. This asymmetry is absent in our data for erbium. It seems likely that this is due to the fact that in erbium the magnetic scattering intensity is dominated by a c-axis-modulated contribution at these temperatures. Thus, the nonresonant magnetic scattering is proportional to $\sin^6\theta$, which is small at these reflections.[11]

III. RESULTS AND DISCUSSIONS

The integrated magnetic intensities of the σ-π (open circles) and σ-σ (solid circles) components of the $(0,0,2+\tau_m)$ reflection were measured as a function of energy near the L_{III} absorption edge of erbium (see Fig. 4). For a pure c-axis modulated (CAM) magnetic structure, it can be shown[10,11] that only the σ-π and π-σ com-

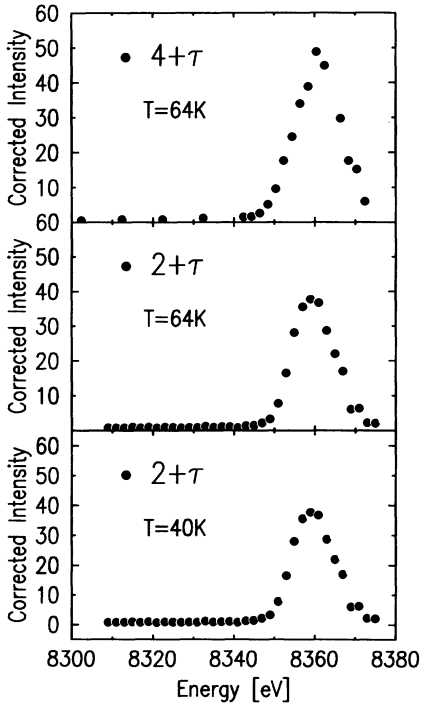

FIG. 3. The integrated intensity of the magnetic satellites (arbitrary units) $(0,0,2+\tau_m)$ and $(0,0,4+\tau_m)$ at 40 and 64 K as a function of the incident x-ray energy near the L_{III} edge. The data are corrected for the variation of absorption coefficient as described in the text.

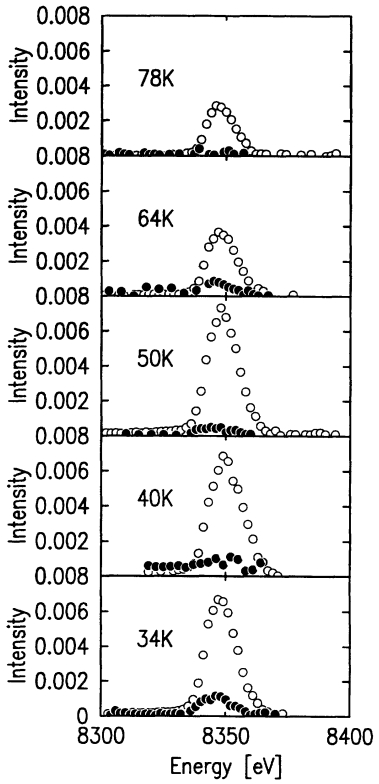

FIG. 4. The integrated magnetic scattering intensities (arbitrary units) of the σ- (solid circles) and π- (open circles) polarized components for the $(0,0,2+\tau_m)$ reflection at various temperatures as a function of the incident x-ray energy, uncorrected for the absorption.

ponents are allowed in the resonant magnetic scattering. By extending our earlier discussions of Eqs. (2)–(4), and neglecting π-σ scattering in Eq. (3) as compared to strong σ-π scattering for a CAM magnetic structure, we can write the intensity obtained in the σ channel as

$$I_\sigma = |f_{\pi\text{-}\sigma}|^2 + \cos^2(2\phi) I_\pi \ . \tag{5}$$

Here again the second term arises from the "leakage" due to the imperfectly set scattering angle of the polarization analyzer ($2\phi \neq 90°$), while the first term represents the contribution of a small π component of the incident beam. It is important to note that these two terms together put an upper limit on the leakage of 6% of the magnetic scattering intensity in the π channel at $(0,0,2+\tau_m)$. The intensity ratio of the π and σ components at 78 K, where the magnetic structure is known to be pure CAM, is again consistent with this leakage calculation. The observed intensities for the σ-σ component are always very weak in comparison to σ-π component, except for the data at 34 K, where the peak intensity of the σ-σ components becomes $\sim\frac{1}{5}$ of the σ-π component. This is quite high considering the leakage estimate given in Eq. (5), and we shall discuss the fitting of this data later in this section.

We show the absorption corrected σ-π components of the magnetic scattering at $(0,0,2+\tau_m)$ versus energy at various temperatures in Fig. 5. We have modeled the energy dependence of these components in erbium by including both nonresonant and resonant contributions for the x-ray-scattering amplitude.[12] We have assumed that the observed magnetic scattering intensity arises from contributions from both basal plane and c-axis moments. In particular, it was assumed that the relative magnitudes of these components are determined by the average tilt angle ψ which the magnetic moment makes with the basal plane. The magnetic scattering intensities at different temperatures were then analyzed by keeping this tilt angle as a fitting parameter. Further, we assumed that the resonant contribution to the σ-π components of the cross section arises mainly from electric dipole transitions coupling $2p$ core states and $5d$ conduction-band states. For simplicity, we have also assumed perfectly linear σ polarization of the incident beam. The intensity for the π-polarized component of the magnetic scattering is then

$$I_\pi = A' |\cos\psi f_{\sigma\text{-}\pi}^{\text{basal}} + \sin\psi f_{\sigma\text{-}\pi}^{c\ \text{axis}}|^2 \ , \tag{6}$$

where

$$f_{\sigma\text{-}\pi}^{\text{basal}} = J_{\text{eff}} \frac{\hbar\omega}{mc^2} \sin(2\theta)\sin(\theta) + \frac{\cos\theta}{\Gamma(x-i)} \left[A - \frac{B}{\Gamma(x-i)} \right] \tag{7}$$

and

$$f_{\sigma\text{-}\pi}^{c\ \text{axis}} = J_{\text{eff}} \frac{\hbar\omega}{mc^2} \sin^3(\theta) - \frac{i\sin\theta}{\Gamma(x-i)} \left[A - \frac{B}{\Gamma(x-i)} \right] . \tag{8}$$

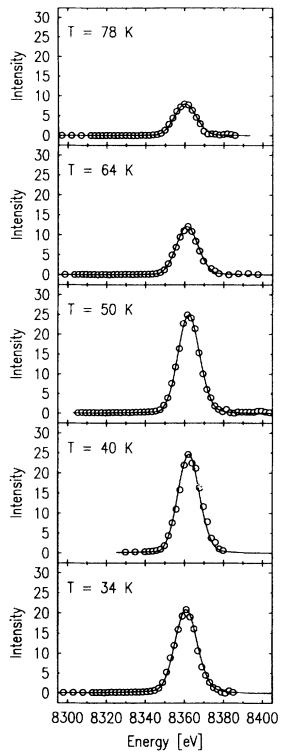

FIG. 5. Integrated magnetic scattering intensities (arbitrary units) of the π-polarized component (open circles) for the $(0,0,2+\tau_m)$ reflection at various temperatures, corrected for the absorption. The solid lines are the results of fits discussed in the text.

In the above expressions, the terms containing J_{eff} are the π-polarized components of the nonresonant contribution to the magnetic scattering. The terms containing A and B are the resonant contributions from electric-dipole transitions coupling $2p$ and $5d$ orbitals.[10,12] $x = 2(E_a - E_b - \hbar\omega)/\Gamma$ is the resonant denominator, with E_a and E_b the initial and ionic excited-state energies, respectively. Γ is the total energy width for all radiative and nonradiative decays from b to a. $\hbar\omega$ is the incident photon energy. The resultant calculated intensities obtained from Eq. (6) were folded with a Gaussian resolution function (with 10 eV FWHM) to obtain the calculated curves (shown in the solid line in Fig. 5). The amplitude A' was determined by fitting the data at 78 K, keeping the tilt angle fixed at 90° (pure c-axis-modulated phase). It was found to be 230. The value of J_{eff} in the above equations was determined from $J_{\text{eff}} = (\frac{2}{3} f_L + \frac{1}{6} f_S) J$, with f_L and f_S obtained from published values[16] and $J = \frac{15}{2}$ for erbium. For the $(0,0,2+\tau_m)$ reflection, this gives $J_{\text{eff}} = 5.5\mu_B$. The values of A, B, and Γ were taken to be 2, 16, and 6, respectively. These values gave reasonable fits and are qualitatively consistent with the values taken for holmium.[12] It should be noted, however, that the fitting of these lines shapes does not determine the parameters uniquely due to high correlation among them, nor do we attribute particular significance to their values.

Once chosen, these parameters were kept fixed for all other temperatures and least-squares fitting was performed by varying only the tilt angle ψ. Reasonable fits were obtained with the tilt angles $\psi=90°$ at 78 K, $\psi=76°$ at 64 K and ψ between 60 and 65° at and below 50 K. In contrast to earlier neutron-diffraction measurements, these results suggest a non-ninety degree tilt angle at 64 K in the c-axis modulated phase. However, it should be noted that no account has been taken of the temperature dependence of the staggered magnetization between 89 and 52 K. Including the latter in the fitting, which is equivalent to letting A' vary with the temperature,[15] leads to the values ($A'=230, \psi=90°$) at 78 K, ($A'=347$, $\psi=90°$) at 64 K and ($A'=347, \psi$ between 65 and 70°) at and below 50 K. The results of these fits are shown by the solid lines in Fig. 5. They are indistinguishable from those obtained by varying only the tilt angle. In view of the number of parameters used in the fitting and the uncertainty of their values, we regard our results as suggestive, but not conclusive. Other models of the magnetic structure of erbium, including the wobbly cycloidal model proposed recently,[8] may also be consistent with our data.

We have used a similar model to fit the σ-σ line shape obtained at 34 K (see Fig. 4). Assuming that this scattering corresponds to the electric quadrupole contribution of the basal plane magnetic structure ($2p \rightarrow 4f$), the intensity for the σ-polarized component of the magnetic scattering can be written[12]

$$I_\sigma = A'' \left| \cos\psi \left[S_{\text{eff}} \frac{\hbar\omega}{mc^2} \sin(2\theta) + \frac{C \sin(2\theta)}{\Gamma(x'-i)} \right] \right|^2 , \qquad (9)$$

where $S_{\text{eff}}=\frac{1}{6}f_S J$ and is equal[16] to 1.03 at the $(0,0,2+\tau_m)$ reflection. Similar to the case of holmium,[12] we find a red shift in the peak position of the σ-σ scattering by 8 eV as compared to that observed in the σ-π scattering. The resultant resonant denominator is then $x'=2(E_a-E_b-\hbar\omega-8)/\Gamma$. The parameters C and A'' were found to be 2.75 and 114, respectively (see Fig. 6).

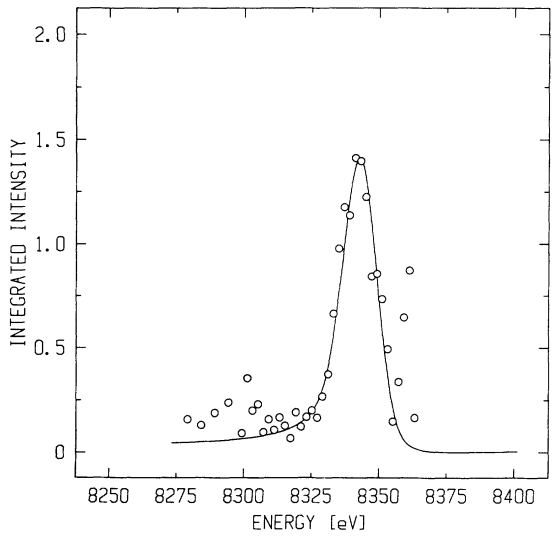

FIG. 6. Integrated magnetic scattering intensities (arbitrary units) of the σ-polarized component (open circles) for the $(0,0,2+\tau_m)$ reflection at 34 K. The solid line is the result of a fit discussed in the text.

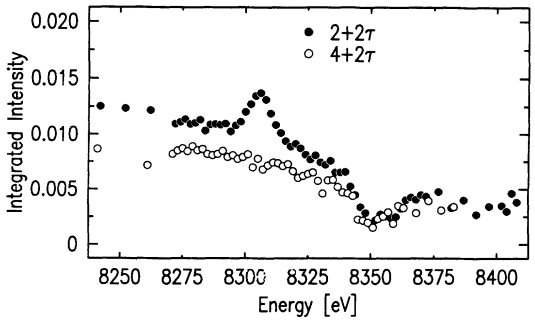

FIG. 7. Integrated intensities (arbitrary units) for the satellites at $(0,0,2+2\tau_m)$ and $(0,0,4+2\tau_m)$ at 34 K as the incident x-ray energy is tuned through the L_{III} edge.

Finally, we show in Fig. 7, the x-ray-scattering cross section for the peaks at $(0,0,2+2\tau_m)$ and $(0,0,4+2\tau_m)$ taken at 34 K as a function of photon energy. The scattering cross section at $(0,0,4+2\tau_m)$ behaves like a charge scattering peak in that the cross section goes through a dip at the absorption edge. The cross section for $(0,0,2+2\tau_m)$, however, is different. Apart from the dip at the edge, characteristic of charge scattering, a peak in the cross section about 80 eV below the absorption edge is also observed. This result is not understood. It may simply involve multiple scattering, or may be related to the anomalous behavior of the magnetic cross section observed in the conical phase, and discussed below.

IV. THE LOW-TEMPERATURE PHASE

In this section, we briefly summarize some features of the measurements obtained below 18 K. We report partial results here in the hope of generating some new ideas, either regarding the low-temperature magnetic structure of erbium or regarding possible multiple-scattering effects. According to the conventional view, the magnetic structure of erbium below 18 K is conical with a net ferromagnetic component along c axis.[5] Abrupt changes in both the c-axis and basal plane lattice constants occur along with this transformation of the magnetic structure. The magnetic wave vector locks to $\tau_m=\frac{5}{21}c^*$ and weak, additional scattering is observed at $2\tau_m=\frac{10}{21}c^*$ and $\tau_s=\frac{2}{7}c^*$. In our measurements, the radial width of the magnetic scattering at the $(0,0,2+\tau_m)$ reflection increased from the resolution width of $0.0015c^*$ at 25 K to $0.02c^*$ below 18 K. This corresponds to a correlation length of order 100 Å, and suggests that the magnetic structure is disordered. In this regard, it is interesting to note that the conical phase is suppressed in erbium thin films,[17] where the in-plane lattice constant is "clamped" at the erbium-substrate interface.

The integrated intensity of the scattering at the magnetic wave vector $(0,0,2+\tau_m)$ below 18 K is shown as a function of energy in Fig. 8. It is clear from this figure that the variation of the magnetic cross section as a function of energy is totally different from that observed in

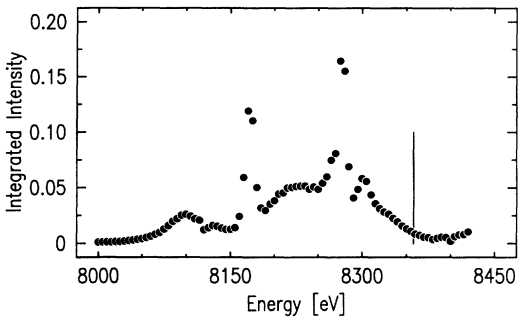

FIG. 8. As-measured integrated intensity (arbitrary units) for the $(0,0,2+\tau_m)$ reflection at 12 K as a function of the incident photon energy. The vertical solid line indicates the position of the $L_{\rm III}$ absorption edge.

higher-temperature phases as discussed in the previous sections. In particular, below 18 K the cross section does not exhibit a single peak described by a Lorentzian squared line shape [refer to Eqs. (6)–(9)] at the $L_{\rm III}$ absorption edge as happens in the other magnetic phases (refer to Fig. 5). Instead, we observe a series of sharp peaks and broad humps extending as far as 2 KeV below the absorption edge. It should be stated here that we performed temperature recycling several times to confirm that the features in Fig. 8 show up only below 18 K. We also performed polarization analysis of the scattered beam and found that most of the sharp features shown in the Fig. 8 appear in the σ-σ channel. These results indicate the possibility of charge scattering at the magnetic wave vector either through multiple scattering or perhaps due to an additional lattice modulation, or both. It is interesting that similar anomalous behavior of the magnetic scattering cross section was observed[18] recently in an independent study of Er-Ho alloys below the $L_{\rm III}$ absorption edge of erbium. Further, in recent neutron-scattering measurements,[4] the hcp-forbidden (111) nuclear peak was observed in this magnetic phase of erbium. It has been argued[4] that this peak is nonmagnetic in nature and indicates lowering of the hcp symmetry, presumably induced by the magnetostrictive effects. However, none of these effects has yet been convincingly explained.

V. CONCLUSIONS

We have presented a synchrotron x-ray-scattering study of the polarization and resonance properties of the magnetic cross section of erbium at various temperatures. A significant enhancement in the intensity of σ-π scattering for the magnetic peaks was observed when the x-ray energy was tuned near the $L_{\rm III}$ absorption edge. This resonant enhancement occurs in all the magnetic phases above 18 K. The energy dependence of the magnetic scattering of erbium near the $L_{\rm III}$ absorption edge has been analyzed using a simple model based on electric dipole and quadrupole transitions coupling $2p$ to $5d$ and $4f$ atomic orbitals. We assumed that the observed magnetic cross section arises from contributions from both basal plane and c-axis moments and that their relative amplitude is determined by the average tilt angle of the magnetic moment. By performing a systematic fitting of the line shape of the magnetic cross section at five different temperatures above 18 K, we obtained values of the tilt angles, versus temperature. An unusual energy dependence of the magnetic cross section below 18 K was also observed. Its origin is not understood. Further studies of erbium are required to understand both the structural changes and anomalous behavior of the magnetic scattering cross section as a function of energy.

ACKNOWLEDGMENTS

We have benefited from discussions with M. Blume, J. Borchers, R. A. Cowley, J. P. Hannon, G. Helgesen, J. Jensen, A. R. Mackintosh, D. Pengra, and G. T. Trammell. This work was supported by the U.S. Department of Energy, Division of Materials Sciences under Contract No. DE-AC02-76CH00016. M.K.S. acknowledges the support of the Bhaba Atomic Research Centre during the preparation of this manuscript. M.W. similarly acknowledges the European Synchrotron Radiation Facility.

APPENDIX

We discuss in this appendix the procedure adopted to calculate the absorption coefficient as a function of energy near the $L_{\rm III}$ absorption edge from the fluorescence data. As mentioned earlier, the procedure was tested using a data set of holmium, where the measured values of both the absorption coefficient and the fluorescence as a function of energy were available. Generally these procedures are difficult, at best, and may produce erroneous results, for example, if two absorption edges are involved. It is always advisable, instead, to use the measured absorption coefficient as a function of energy for performing quantitative analysis of the line shapes of the magnetic scattering near an absorption edge. We regard the results of the fits to these line shapes, therefore, as qualitative. Under assumption of proportionality, one can write the calculated absorption coefficient $\mu^C(E)$ as a function of energy

$$\mu^C(E)=\mu_L+\Delta\mu^C(E)\ , \tag{A1}$$

where

$$\Delta\mu^C(E)=\frac{\mu H-\mu L}{F_H-F_L}[F(E)-F_L]\ .$$

In the above equation $\Delta\mu^C(E)$ represents the calculated change in the absorption coefficient near the absorption edge. F_H and F_L are the measured background (fluorescence) above and below the absorption edge. Similarly, μ_H and μ_L are known absorption coefficients well above and below the absorption edge. In Fig. 9, the dotted curve was obtained from the measured background, $F(E)$, using Eq. (1), and the circles represent the mea-

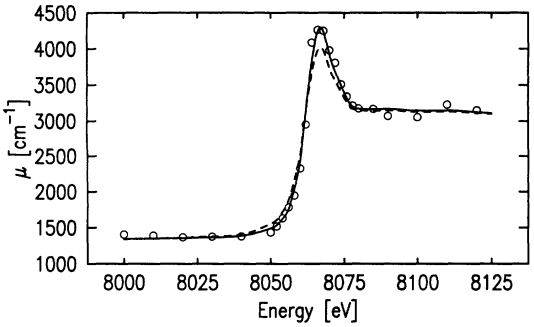

FIG. 9. The absorption coefficient of holmium plotted as a function of energy around the L_{III} edge, measured from a 5-μm film (open circles) and calculated using Eq. (A1) (dashed line) and Eq. (A2) (solid line).

sured absorption coefficient. The agreement can be improved if we consider the fact that not all of the fluorescence photons generated at the sample reach the detector. For a fixed penetration depth T, the total number of fluorescence photons generated will be proportional to $[1-\exp(-\mu T)]F$ at any fixed energy. The prefactor used here compensates for the fact that as μ increases more photons get absorbed in the same depth T and, as a result, more fluorescent photons are generated. With this modification Eq. (1) can be written as

$$\Delta\mu^C(E)=\frac{\mu H-\mu L}{F_H-F_L}[F(E)-F_L]\frac{1-\exp[-\mu^C(E)T]}{1-\exp(-\mu_H T)} \quad . \tag{A2}$$

The solid curve shown in Fig. 9 was obtained from Eq. (2) by using $T=5\mu$, which gives 80% absorption for μH within that thickness. $\mu^C(E)$ in the numerator of Eq. (2) were obtained from the calculated values of Eq. (1). The resultant agreement is satisfactory.

We used these procedures in the present study of erbium to calculate the absorption coefficient as a function of energy near the L_{III} absorption edge (8358 eV) by using known values of μL and μH and by choosing a T of 5μm, which gives 80% absorption for μH of erbium.

*Present address: Bhabha Atomic Research Centre, Solid State Physics Division, Bombay 400 085, India.

†Present address: European Synchrotron Radiation Facility, B.P. 220, F-38043, Grenoble Cedex, France.

[1]J. W. Cable, E. O. Wollan, W. C. Koehler, and M. K. Wilkinson, Phys. Rev. **140**, A1896 (1965).

[2]M. Habenschuss, C. Stassis, S. K. Sinha, H. W. Deckman, and F. H. Spedding, Phys. Rev. **B 10**, 1020 (1974).

[3]M. Atoji, Solid State Commun. **14**, 1047 (1974).

[4]H. Lin, M. F. Collins, T. M. Holden, and W. Wei, Phys. Rev. B **45**, 12 873 (1992); H. Lin, M. F. Collins, T. M. Holden, and W. Wei, J. Magn. Magn. Mater. **104-107**, 1511 (1992).

[5]D. Gibbs, J. Bohr, J. D. Axe, D. E. Moncton, and K. L. D'Amico, Phys. Rev. B **34**, 8182 (1986).

[6]J. Bohr, D. Gibbs, D. E. Moncton, and K. L. D'Amico, Physica **A 140**, 349 (1986).

[7]J. Jensen and A. R. Mackintosh, *Rare Earth Magnetism: Structure and Excitations* (Oxford University Press, Oxford, 1991).

[8]R. A. Cowley and J. Jensen, J. Phys. **C 4**, 9673 (1992); J. Jensen and R. A. Cowley, Europhys. Lett. **21**, 705 (1993); for studies in a magnetic field, see also, D. F. McMorrow, D. Jehan, R. A. Cowley, R. S. Eccleston, and G. J. McIntyre, J. Phys. **C 4**, 8599 (1992).

[9]D. Gibbs, D. R. Harshman, E. D. Isaacs, D. B. McWhan, D. Mills, and C. Vettier, Phys. Rev. Lett. **61**, 1241 (1988).

[10]J. P. Hannon, G. T. Trammell, M. Blume, and D. Gibbs, Phys. Rev. Lett. **61**, 1245 (1988).

[11]J. Bohr, D. Gibbs, and K. G. Huang, Phys. Rev. **B 42**, 4322 (1990).

[12]D. Gibbs, G. Grübel, D. R. Harshman, E. D. Isaacs, D. B. McWhan, D. Mills, and C. Vettier, Phys. Rev. **B 43**, 5663 (1991).

[13]D. Gibbs, M. Blume, D. R. Harshman, and D. B. McWhan, Rev. Sci. Instrum. **60**, 1655 (1989).

[14]M. Blume, J. Appl. Phys. **57**, 3615 (1985); M. Blume and D. Gibbs, Phys. Rev. **B 37**, 1779 (1988).

[15]The increase of A' with decreasing temperature implied from the fitting is qualitatively consistent with recent measurements of the temperature dependence of the order parameter in erbium by G. Helgesen, T. Thurston, J. P. Hill, and D. Gibbs (unpublished).

[16]M. Blume, A. J. Freeman, and R. E. Watson, J. Chem. Phys. **37**, 1242 (1962); **41**, 1878 (1964).

[17]J. A. Borchers, M. B. Salamon, R. W. Erwin, J. J. Rhyne, R. R. Du, and C. P. Flynn, Phys. Rev. B **43**, 3123 (1991); J. A. Borchers *et al.*, *ibid.* **44**, 11 814 (1991).

[18]D. Pengra, N. Toft, F. Fiedenhans'l, M. Wulff, and J. Bohr (unpublished).